Investigation of magnetic order in SmTr_{2}Zn_{20} (Tr=Fe,Co,Ru) and SmTr_{2}Cd_{20} (Tr=Ni,Pd)

D. Yazici, B. D. White, P.-C. Ho, N. Kanchanavatee, K. Huang, A. J. Friedman, A. S. Wong, V. W. Burnett, N. R. Dilley, and M. B. Maple

Phys. Rev. B **90**, 144406 — Published 3 October 2014

DOI: 10.1103/PhysRevB.90.144406

Investigation of magnetic order in SmTr_2Zn$_{20}$ (*Tr* = Fe, Co, Ru) and SmTr_2Cd$_{20}$ (*Tr* = Ni, Pd)

D. Yazici[1,2], B. D. White[1,2], P.-C. Ho[5], N. Kanchanavatee[1,2], K. Huang[1,2,3], A. J. Friedman[1,2], A. S. Wong[1,2], V. W. Burnett[1,2], N. R. Dilley[4], and M. B. Maple[1,2,3*]

[1]*Department of Physics, University of California, San Diego, La Jolla, California 92093, USA*

[2]*Center for Advanced Nanoscience, University of California, San Diego, La Jolla, California 92093, USA*

[3]*Materials Science and Engineering Program, University of California, San Diego, La Jolla, California 92093, USA*

[4]*Quantum Design, 6325 Lusk Boulevard, San Diego, California 92121, USA and*

[5]*Department of Physics, California State University Fresno, Fresno, California 93740, USA*

(Dated: September 16, 2014)

Single crystals of the "cage compounds" SmTr_2Zn$_{20}$ (*Tr* = Fe, Co, Ru) and SmTr_2Cd$_{20}$ (*Tr* = Ni, Pd) have been investigated by means of electrical resistivity, magnetization, and specific heat measurements. The compounds SmFe$_2$Zn$_{20}$, SmRu$_2$Zn$_{20}$, and SmNi$_2$Cd$_{20}$ exhibit ferromagnetic order with Curie temperatures of T_C = 47.4 K, 7.6 K, and 7.5 K, respectively, whereas SmPd$_2$Cd$_{20}$ is an antiferromagnet with a Néel temperature of T_N = 3.4 K. No evidence for magnetic order is observed in SmCo$_2$Zn$_{20}$ down to 110 mK. The Sommerfeld coefficients γ are found to be 57 mJ/mol-K^2 for SmFe$_2$Zn$_{20}$, 79.5 mJ/mol-K^2 for SmCo$_2$Zn$_{20}$, 258 mJ/mol-K^2 for SmRu$_2$Zn$_{20}$, 165 mJ/mol-K^2 for SmNi$_2$Cd$_{20}$, and 208 mJ/mol-K^2 for SmPd$_2$Cd$_{20}$. Enhanced values of γ and a quadratic temperature dependence of the electrical resistivity at low temperature for SmRu$_2$Zn$_{20}$ and SmPd$_2$Cd$_{20}$ suggest an enhancement of the quasiparticle masses due to hybridization between localized 4f and conduction electron states.

PACS numbers: 71.27.+a, 72.15.Eb, 75.30.Mb, 75.50.Cc

I. INTRODUCTION

Intermetallic compounds containing Sm have attracted significant interest for displaying a large variety of unusual physical phenomena. For example, SmS undergoes an isostructural first order electronic phase transition to a collapsed gold phase that exhibits "valence fluctuation" behavior,[1,2] the La$_{1-x}$Sm$_x$Sn$_3$ system displays Kondo anomalies in superconducting and normal state properties[3,4] and SmB$_6$ has an intermediate Sm valence and is a hybridization gap semiconductor (aka, Kondo insulator).[5] Among the Sm-based filled skutterudite compounds, SmOs$_4$Sb$_{12}$ displays a heavy fermion state that is robust against applied magnetic field,[6–10] SmFe$_4$P$_{12}$ exhibits ferromagnetic order,[11] and SmRu$_4$P$_{12}$ undergoes a metal-insulator transition associated with multipolar order.[12]

The class of intermetallic compounds, RTr_2X_{20} (R = rare earth, Tr = transition metal, and X = Al, Zn, Cd), crystallizes in the CeCr$_2$Al$_{20}$-type ($Fd\bar{3}m$ space group) cubic structure.[13–17] These RTr_2X_{20} compounds have recently attracted much attention because of their unique crytal structure, in which R ions are encapsulated in the Frank-Kasper cages formed by 16 X ions, and have a larger coordination number of tetrahedral groupings of spheres,[18] compared to the filled skutterudites and rare-earth hexaborides.[19–30] This crystal structure provides an opportunity to study strongly correlated electronic states, which can be associated with either f or d electrons, and localized rare-earth magnetic moments that have a large spatial separation.

The only Sm-based RTr_2X_{20} compounds to be characterized in single-crystalline form are SmTr_2Al$_{20}$ (Tr = Ti, V, Cr), which order antiferromagnetically and show heavy fermion behavior with strong Sm valence fluctuations.[31,32] In order to better understand the SmTr_2X_{20} compounds, we examined the thermodynamic and electrical transport properties of four previously unreported compounds: SmTr_2Zn$_{20}$ (Tr = Fe, Ru) and SmTr_2Cd$_{20}$ (Tr = Ni, Pd) together with SmCo$_2$Zn$_{20}$. X-ray diffraction (XRD), electrical resistivity, magnetization, and specific heat measurements revealed a ferromagnetic ground state for SmFe$_2$Zn$_{20}$, SmRu$_2$Zn$_{20}$, and SmNi$_2$Cd$_{20}$ and an antiferromagnetic ground state for SmPd$_2$Cd$_{20}$. The formation of heavy quasiparticles in the ordered states of the SmRu$_2$Zn$_{20}$ and SmPd$_2$Cd$_{20}$ compounds is also observed. Analysis of the low-temperature electrical resistivity data suggests the presence of spin-wave excitations for SmFe$_2$Zn$_{20}$, SmRu$_2$Zn$_{20}$, SmNi$_2$Cd$_{20}$, and SmPd$_2$Cd$_{20}$.

II. EXPERIMENTAL DETAILS

Single crystals of SmTr_2Zn$_{20}$ (*Tr* = Fe, Co, Ru), YFe$_2$Zn$_{20}$, SmTr_2Cd$_{20}$ (*Tr* = Ni, Pd), YNi$_2$Cd$_{20}$, and LaNi$_2$Cd$_{20}$ were prepared by the Zn and Cd-self flux methods, respectively. Details of the sample synthesis are described in Refs. 22 and 33. Crystal structure and sample quality were primarily characterized through analysis of powder XRD patterns collected by a Bruker D8 x-ray diffractometer. Four-wire electrical resistivity measurements were performed from 300 K to ∼1.1 K in a pumped ^{4}He Dewar for SmTr_2Zn$_{20}$ (*Tr* = Fe, Co, Ru) and SmPd$_2$Cd$_{20}$, and down to 110 mK using a ^{3}He-^{4}He dilution refrigerator for SmCo$_2$Zn$_{20}$. Electrical resistivity measurements were performed for SmNi$_2$Cd$_{20}$ down to 0.36 K using an electrical transport option on the ^{3}He insert for a Quantum Design Physical Property Measurement System (PPMS) equipped with a 9 T superconducting magnet. Magnetization measurements were performed between 300 K and 2 K in a Quantum Design Magnetic Property Measurement System (MPMS) equipped with a 7 T superconducting magnet. Specific heat measurements were performed down to 1.8 K in a PPMS Dynacool using a standard thermal relaxation technique. The orientation of single crystals was determined using a Bruker D8 Discover x-ray diffractometer.

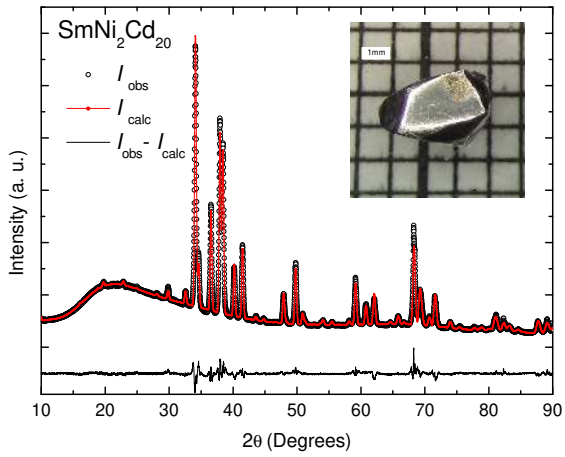

FIG. 1: X-ray diffraction pattern for $SmNi_2Cd_{20}$ measured at room temperature. The black open circles indicate the observed intensity I_{obs}, the red line represents the calculated intensity I_{calc}, and the black line indicates the difference $I_{obs} - I_{calc}$. A broad, featureless hump at low angle comes from the glass slide and petroleum jelly used to mount the powder on the slide. A photograph of a $SmNi_2Cd_{20}$ single crystal is shown in the inset of the figure where the small squares are 1 mm x 1 mm for reference.

III. RESULTS AND DISCUSSION

Analysis of powder XRD patterns indicated that the single crystals contained no inclusions of impurity phases. Table I lists the results of Rietveld refinements that were conducted on powder XRD patterns for each sample using GSAS[34] and EXPGUI.[35] The $CeCr_2Al_{20}$-type cubic crystal structure with space group $Fd\bar{3}m$ was observed for all samples. A representative XRD pattern (for the $SmNi_2Cd_{20}$ single crystal) is shown in Fig. 1, plotted with its refined pattern for comparison.

Magnetization divided by applied magnetic field M/H data are displayed as a function of temperature in Fig. 2(a). Measurements were performed in applied magnetic fields of H = 0.1 T for $SmFe_2Zn_{20}$, $SmRu_2Zn_{20}$, and $SmPd_2Cd_{20}$, H = 0.5 T for $SmCo_2Zn_{20}$, and in H = 0.05 T for $SmNi_2Cd_{20}$. The $SmFe_2Zn_{20}$, $SmRu_2Zn_{20}$, $SmNi_2Cd_{20}$, and $SmPd_2Cd_{20}$ compounds exhibit features in M/H that are consistent with a magnetic phase transition. M/H data as a function of temperature reveal the primary difference between the Fe column members ($SmFe_2Zn_{20}$ and $SmRu_2Zn_{20}$) and the Co column member ($SmCo_2Zn_{20}$): for Fe column members, there is an apparent ferromagnetic (FM) order (with notably-high and moderately-high Curie temperature of T_C = 47.4 K and 7.6 K for $SmFe_2Zn_{20}$ and $SmRu_2Zn_{20}$, respectively). In contrast, no evidence for magnetic order is observed down to 2 K for $SmCo_2Zn_{20}$. However, the large increase in M/H below 10 K for $SmCo_2Zn_{20}$, which does not obey Curie-Weiss law behavior, could in principle be related to magnetic order below 2 K.

Among the RTr_2Zn_{20} compounds, $GdFe_2Zn_{20}$ and $GdCo_2Zn_{20}$ have attracted special attention due to the distinct magnetic properties exhibited by each compound.[21,22,36] $GdFe_2Zn_{20}$ is a FM with a remarkably-high Curie temperature of T_C = 86 K compared with other $R Fe_2Zn_{20}$ compounds. However, as Co is substituted for Fe, ferromagnetic order is rapidly suppressed, culminating in antiferromagnetic order at T_N = 5.7 K in $GdCo_2Zn_{20}$.[21,36] Band structure calculations suggest that the enhanced Curie temperature in $GdFe_2Zn_{20}$ is due to a large d-electron contribution to the electronic density of states at the Fermi energy when compared to $GdCo_2Zn_{20}$, and that the transition from FM to AFM order is associated with the filling of electronic states with two additional electrons/f.u.[21,36] $TbFe_2Zn_{20}$ and $TbCo_2Zn_{20}$ also exhibit distinct magnetic behavior according to neutron scattering measurements; $TbFe_2Zn_{20}$ is a ferromagnet with T_C = 66 K and $TbCo_2Zn_{20}$ orders antiferromagnetically at T_N = 2.5 K.[37] The neutron scattering data are consistent with a picture of the $R Fe_2Zn_{20}$ family of compounds in which the high ordering temperatures are associated with the highly polarizable Fe lattice; however, we note that the small magnetic moments on the Fe sites do not order.[37] This distinct magnetic behavior is expected because the rare-earth and transition-metal ions in the RTr_2Zn_{20} compounds are surrounded by Zn cages, preventing direct magnetic exchange interactions between the 4*f* or 3*d* levels. Rather, an indirect Ruderman-Kittel-Kasuya-Yosida (RKKY)[38–41] magnetic exchange interaction, mediated by the conduction electrons, provides the mechanism for magnetic order. Therefore, the conduction electrons play an important role in controlling the magnetic properties of the RTr_2Zn_{20} compounds.

The remarkable differences in magnetic behavior between $SmCo_2Zn_{20}$ and $SmFe_2Zn_{20}$ could be associated with the fact that there are two extra electrons per formula unit in $SmCo_2Zn_{20}$ than in $SmFe_2Zn_{20}$, in analogy with the R = Gd compounds.[21,36] Interestingly, even though Ni and Pd are in the same column of the periodic table, $SmNi_2Cd_{20}$ and $SmPd_2Cd_{20}$ show different magnetic behavior in their ground states; $SmNi_2Cd_{20}$ has a FM-ground state with T_C = 7.5 K and $SmPd_2Cd_{20}$ has an AFM ground state with T_N = 3.4 K.

Inverse dc magnetic susceptibility χ_{dc}^{-1} vs. T data for $SmFe_2Zn_{20}$ and $SmNi_2Cd_{20}$ were fitted using the Curie-Weiss law,

$$\chi - \chi_0 = C_0/(T - \Theta_{CW}), \quad (1)$$

where χ_0 is a temperature-independent contribution from the filled electron shells and conduction electrons, in the temperature range 60 - 300 K to determine the Curie-Weiss temperature Θ_{CW} and effective magnetic moment of the rare earth site μ_{eff}. The effective moment μ_{eff} was extracted from the Curie constant, $C_0 = N_A\mu_{eff}^2/3k_B$, where N_A is Avogadro's number and k_B is Boltzmann's constant. This analysis was performed by fitting Eq. (1) to the data using non-linear least squares regression. The resulting best-fit parameter values for μ_{eff} and Θ_{CW} are tabulated in Table I. The theoretical Sm^{3+} free ion magnetic moment is $\mu_{eff} = g_J[J(J+1)]^{1/2}\mu_B$ = 0.845 μ_B/f.u., where g_J = 0.286 is the Landé g factor and J = 5/2. The effective moment μ_{eff} values were determined to be 1.7 μ_B/f.u. and 0.71 μ_B/f.u. for $SmFe_2Zn_{20}$ and $SmNi_2Cd_{20}$,

TABLE I: Summary of structural, magnetic, and electrical transport properties for SmTr_2Zn$_{20}$ (*Tr* = Fe, Co, Ru) and SmTr_2Cd$_{20}$ (*Tr* = Ni, Pd) compounds. Included in the table are the cubic lattice parameter, a; Curie-Weiss temperature Θ_{CW}; effective magnetic moment μ_{eff}; magnetic ordering temperature T_C or T_N; saturation magnetic moment μ_{sat} at 5 T along the [111] crystallographic direction; residual resistivity, ρ_0, measured at $T \sim 1.2$ K for SmTr_2Zn$_{20}$ (*Tr* = Fe, Co, Ru) and SmPd$_2$Cd$_{20}$, and $T \sim 0.5$ K for SmNi$_2$Cd$_{20}$; coefficient of the T^2 term of the electrical resistivity, A (with temperature range of fit given in parenthesis); residual resistivity ratio, $RRR \equiv R$(300 K)/R(1.2 K) for SmTr_2Zn$_{20}$ (Tr = Fe, Ru) and SmPd$_2$Cd$_{20}$ and $RRR \equiv R$(300 K)/R(0.5 K) for SmNi$_2$Cd$_{20}$ and SmCo$_2$Zn$_{20}$; and spin-wave energy gap, Δ_{spw}.

Compound	a,(Å)	Θ_{CW}, (K)	μ_{eff}, (μ_B)	T_C or T_N, (K)	μ_{sat}, (μ_B)	ρ_0, ($\mu\Omega$cm)	A ($\frac{\mu\Omega\text{cm}}{\text{K}^2}$)	RRR	Δ_{spw} (K)
SmFe$_2$Zn$_{20}$	14.51	47.8	1.7	47.4	1.05	3.5	4.41×10^{-3} ($T < 4$ K)	21	4.82
SmCo$_2$Zn$_{20}$	14.08	-1.83	0.99	–	–	5.8	–	12	–
SmRu$_2$Zn$_{20}$	14.73	8.62	0.71	7.6	0.47	11.5	2.9×10^{-2} ($T < 3$ K)	7.2	3.88
SmNi$_2$Cd$_{20}$	15.53	56.2	0.71	7.5	0.52	0.11	–	21	8.79
SmPd$_2$Cd$_{20}$	15.56	-6.88	0.74	3.4	–	0.06	4.8×10^{-1} ($T < 3$ K)	80	3.63

respectively, which are larger for SmFe$_2$Zn$_{20}$ and somewhat smaller for SmNi$_2$Cd$_{20}$ than the theoretical Sm^{3+} free ion value. It has been reported that DyFe$_2$Zn$_{20}$ is a ferrimagnet with a magnetic moment associated with both Dy and Fe via Mössbauer experiments.[20] This might be the reason for the larger μ_{eff} value of SmFe$_2$Zn$_{20}$: both Sm and Fe may have magnetic moments in this compound. The positive values of Θ_{CW} = 47.8 K for SmFe$_2$Zn$_{20}$ and 56.2 K for SmNi$_2$Cd$_{20}$ are consistent with ferromagnetic interactions. However, the magnitude of Θ_{CW} for SmNi$_2$Cd$_{20}$ is a factor of $\sim$ 7.5 larger than T_C. This observation may suggest the presence of magnetic frustration or a competition between FM and another ordered state in this compound.

On the other hand, χ_{dc}^{-1} vs. T data for SmCo$_2$Zn$_{20}$, SmRu$_2$Zn$_{20}$, and SmPd$_2$Cd$_{20}$ show an extremely weak T dependence with distinctly non-Curie-Weiss behavior. This is common in Sm-containing compounds, since Sm^{3+} ions have relatively low-energy angular momentum excited states above the Hund's rule J = 5/2 ground state. A simple Curie-Weiss law was, therefore, unable to adequately describe the data. Although possible reasons for this weak T dependence include valence fluctuations of Sm ions, the origin is not yet well understood. Similar weak T dependence was also observed in SmTr_2Al$_{20}$ compounds with 3d transition metals.[31,32] Previous work has shown that $\chi(T)$ for Sm compounds can often be reasonably-well described, without considering splitting of the Sm multiplet by the CEF, by the equation,[10,42]

$$\chi(T) = \frac{N_A}{k_B}\left[\frac{\mu_{eff}^2}{3(T-\theta_{CW})} + \frac{\mu_B^2}{\delta}\right], \qquad (2)$$

where μ_B is the Bohr magneton, $\delta = 7\Delta/20$, and Δ is the energy (expressed in units of K) between the Hund's rule $J = 5/2$ ground state and the $J = 7/2$ first excited state. Equation (2) consists of a Curie-Weiss term due to the $J = 5/2$ ground-state contribution and a temperature-independent Van Vleck term due to coupling with the first excited $J = 7/2$ multiplet. The best overall fit of Eq. (2) to the $\chi_{dc}^{-1}(T)$ data, is shown in Fig. 2(b) (dashed black lines). It can be seen that the free-ion Van Vleck term, without adding a Pauli paramagnetic term, provides an excellent fit to the temperature-independent region at high temperatures. The contribution below 100 K displays Curie-Weiss behavior and fits yield μ_{eff} values of 0.99 μ_B/f.u., 0.71 μ_B/f.u., and 0.74 μ_B/f.u. with Θ_{CW} values of -1.83 K, 8.62 K, and -6.88 K for SmCo$_2$Zn$_{20}$, SmRu$_2$Zn$_{20}$, and SmPd$_2$Cd$_{20}$, respectively. The sign of the Θ_{CW} values are consistent with ferromagnetic interactions in SmRu$_2$Zn$_{20}$ (T_C = 7.6 K) and antiferromagnetic interactions in SmPd$_2$Cd$_{20}$ (T_N = 3.4 K). The signs of Θ_{CW} for SmCo$_2$Zn$_{20}$ implies that there are weak antiferromagnetic interactions in that compound, which is consistent with previous reports.[19,22] However, there are deviations in the μ_{eff} values from the free-ion effective paramagnetic moment of 0.845 μ_B/f.u. We obtain a larger value for SmCo$_2$Zn$_{20}$ and smaller values for SmRu$_2$Zn$_{20}$ and SmPd$_2$Cd$_{20}$. The resulting Δ values are 412 K, 265 K, and 1488 K for SmCo$_2$Zn$_{20}$, SmRu$_2$Zn$_{20}$, and SmPd$_2$Cd$_{20}$, respectively. These values for SmCo$_2$Zn$_{20}$ and SmRu$_2$Zn$_{20}$ are much lower than the $\Delta \sim$ 1500 K value estimated for free Sm^{3+} ions.[43] However, low values of Δ have previously been inferred from the fits to $\chi_{dc}(T)$ data for other Sm-based compounds such as SmRh$_4$B$_4$ (Δ = 1080 K) and SmOs$_4$Sb$_{12}$ (Δ = 850 K).[10,42]

The nature of the magnetic order in these compounds was further studied by measurements of the isothermal magnetization at low temperatures. Magnetization M vs. H data, measured at 2 K with H parallel to the [111] direction, are presented in Fig. 2(c). For SmFe$_2$Zn$_{20}$, SmRu$_2$Zn$_{20}$, and SmNi$_2$Cd$_{20}$, $M(H)$ is consistent with a FM state with a rapid rise and saturation of the ordered moment as the magnetic field increases. By extrapolating the high-field slope of the magnetization curves at 2 K back to H = 0 T, the saturation moment μ_{sat} was determined to be 1.05 μ_B/f.u. for SmFe$_2$Zn$_{20}$; this value is higher than the theoretical value of $M_{sat} = g_J J\mu_B$ = 0.71 μ_B/f.u. We also obtain values of 0.47 μ_B/f.u. and 0.52 μ_B/f.u., for SmRu$_2$Zn$_{20}$ and SmNi$_2$Cd$_{20}$, respectively, which are $\sim 70\%$ of the theoretical value of the free Sm^{3+} ion. The ratio of the effective magnetic moment to the saturation magnetic moment for these compounds is $\mu_{eff}/\mu_{sat} \sim 1$, indicating that the f electrons associated with the Sm magnetic moments are localized.[44] At 2 K, the remnant magnetization M_R is 0.58 μ_B/f.u., 0.31 μ_B/f.u., and 0.27 μ_B/f.u. for SmFe$_2$Zn$_{20}$, SmRu$_2$Zn$_{20}$, and SmNi$_2$Cd$_{20}$,

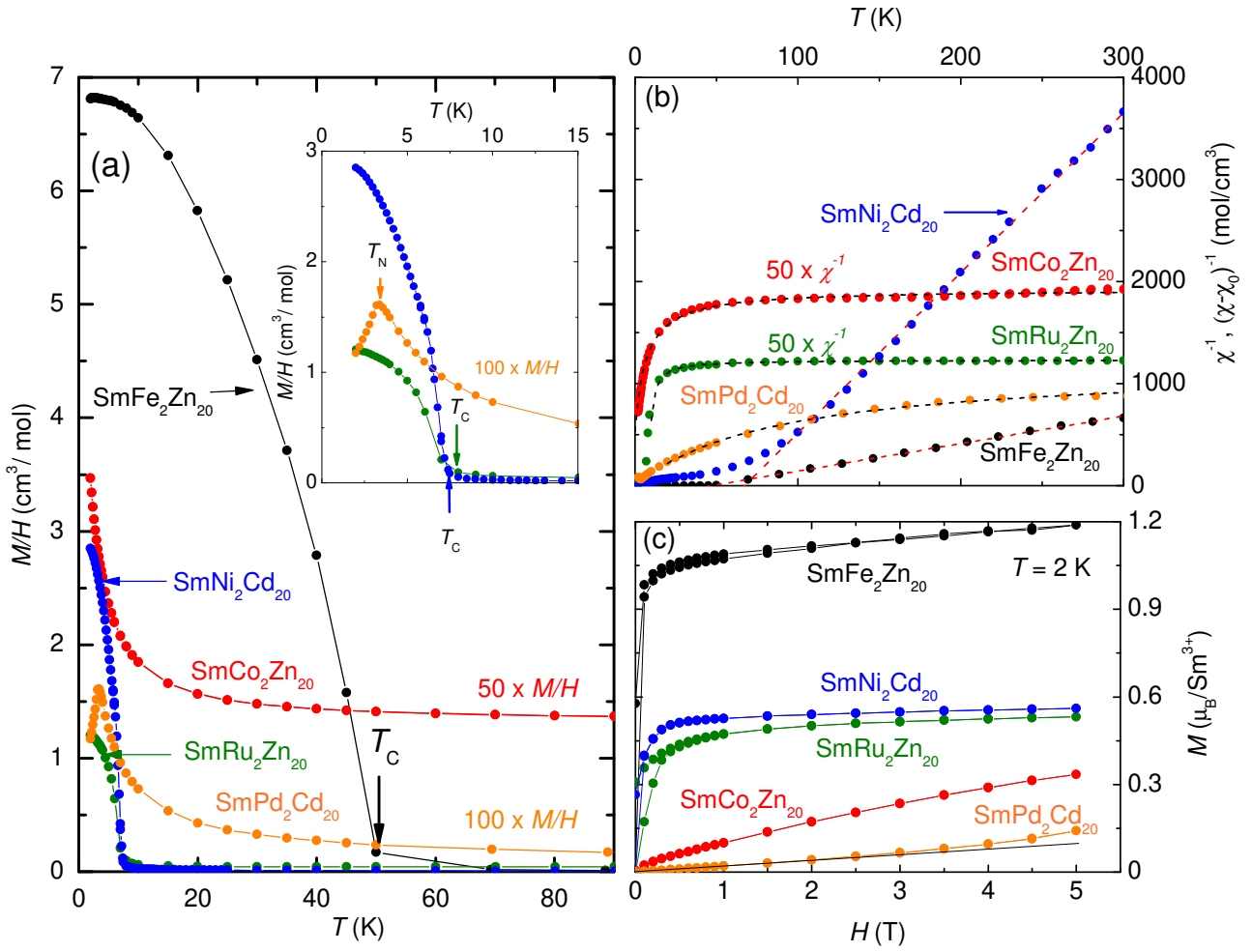

FIG. 2: (a) Magnetic susceptibility, M/H, as a function of temperature, T, measured in an applied magnetic field of H = 0.1 T for $SmFe_2Zn_{20}$, $SmRu_2Zn_{20}$, and $SmPd_2Cd_{20}$, H = 0.5 T for $SmCo_2Zn_{20}$, and H = 0.05 T for $SmNi_2Cd_{20}$. Inset: Low temperature M/H vs. T data for $SmRu_2Zn_{20}$, $SmNi_2Cd_{20}$, and $SmPd_2Cd_{20}$. The magnetic ordering temperatures, T_C and T_N, are emphasized by arrows. The M/H vs. T data for $SmCo_2Zn_{20}$ and $SmPd_2Cd_{20}$ were scaled by factors of 50 and 100, respectively, for clarity. (b) Inverse magnetic susceptibility data, $\chi^{-1} = H/M$ vs. T, for SmTr_2Zn_{20} (Tr = Fe, Co, Ru) and SmTr_2Cd_{20} (Tr = Ni, Pd). Dashed red lines represent modified Curie-Weiss fits to the data using Eq. (1) and dashed black lines represent the fits to the data using Eq. (2) as described in the text. The $\chi^{-1} = H/M$ vs. T data for $SmCo_2Zn_{20}$ and $SmRu_2Zn_{20}$ were scaled by a factor of 50 for clarity. (c) M vs. H data at T = 2 K for the SmTr_2Zn_{20} (Tr = Fe, Co, Ru) and SmTr_2Cd_{20} (Tr = Ni, Pd) compounds. The black solid line is a guide to the eye to clarify the separation from the linear behavior of M vs. H data for $SmPd_2Cd_{20}$ at an applied magnetic field of H = 2.5 T.

respectively. The $M(H)$ isotherms at temperatures higher than their respective T_C's, (not shown here) are approximately linear. On the other hand, M vs. H data measured at 2 K are hysteretic for $SmFe_2Zn_{20}$, $SmRu_2Zn_{20}$, and $SmNi_2Cd_{20}$; however, positive curvature for $SmCo_2Zn_{20}$, which cannot be described by Brillouin function and approximately linear behavior for $SmPd_2Cd_{20}$ up to H = 2.5 T are consistent with AFM correlations which can be field-stabilized to fully saturated states in large enough applied magnetic fields. A magnetic field of H = 5 T was unable to saturate the magnetic moments of the $SmCo_2Zn_{20}$ and $SmPd_2Cd_{20}$ compounds. There is a departure from the linear behavior of M vs. H data for $SmPd_2Cd_{20}$ at an applied magnetic field of H = 2.5 T, which may be related with classical spin reorientation in a cubic symmetry coordination (i.e., an incipient metamagnetic phase transition).

The electrical resistivity ρ vs. temperature T data for the SmTr_2Zn_{20} (Tr = Fe, Co, Ru) and $SmNi_2Cd_{20}$ compounds are displayed in Fig. 3. Metallic behavior is observed for all of the compounds. The zero-field residual resistivity ratios, $RRR \equiv R(300\ \mathrm{K})/R(1.2\ \mathrm{K})$ for SmTr_2Zn_{20} (Tr = Fe, Ru) and $SmPd_2Cd_{20}$, $RRR \equiv R(300\ \mathrm{K})/R(0.05\ \mathrm{K})$ for $SmNi_2Cd_{20}$, and $RRR \equiv R(300\ \mathrm{K})/R(0.11\ \mathrm{K})$ for $SmCo_2Zn_{20}$ were found to be $\sim$ 7-80, which indicates that the single crystals studied are of good metallurgical quality (i.e., low impurity scattering). The values for RRR are given in Table I. A shoulder develops in the zero-field $\rho(T)$ curve for $SmFe_2Zn_{20}$, $SmRu_2Zn_{20}$, $SmNi_2Cd_{20}$, and $SmPd_2Cd_{20}$, be-

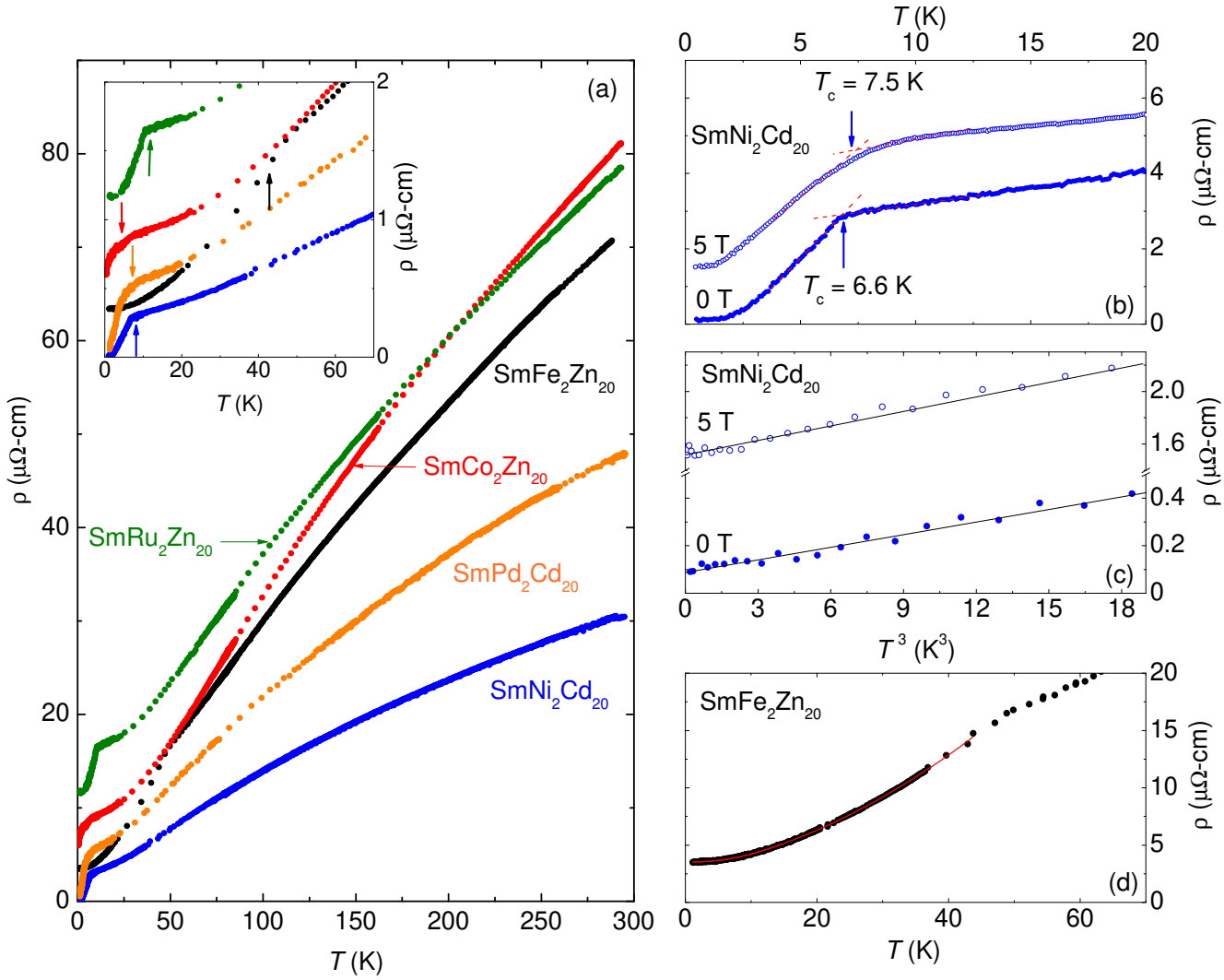

FIG. 3: (a) Electrical resistivity, ρ, vs. temperature, T, for SmTr_2Zn$_{20}$ (Tr = Fe, Co, Ru) and SmTr_2Cd$_{20}$ (Tr = Ni, Pd). Inset: Electrical resistivity at low temperatures emphasizing the magnetic ordering temperatures, T_C and T_N (indicated by arrows). For SmCo$_2$Zn$_{20}$, the arrow indicates the low-temperature shoulder in $\rho(T)$. (b) Low-T ρ vs. T data in zero field and an H = 5 T applied magnetic field for SmNi$_2$Cd$_{20}$. The red dashed lines indicate the method we used to determine T_C. (c) Low-T ρ vs. T^3 data in zero field and an H = 5 T applied magnetic field for SmNi$_2$Cd$_{20}$ with power-law fits (solid black line). (d) Low-T ρ vs. T data in zero magnetic field for SmFe$_2$Zn$_{20}$ with spin-wave scattering fit (solid red line) using Eq. (3).

low which, $\rho(T)$ exhibits a sharp drop, indicating a transition to an ordered state. A similar shoulder with a gentle roll off can also be seen in the zero-field $\rho(T)$ curve for SmCo$_2$Zn$_{20}$ (indicated by an arrow in the inset of Fig. 3(a)) without an accompanying sharp drop. The transition temperatures T_C and T_N at which these drops occur are defined as the intercept of two lines, one of which is a linear fit to the data above the transition, while the other is a linear fit to the data below the transition. Examples of this definition of the T_C values are shown in Fig. 3(b) and the resulting values of T_C and T_N are indicated by arrows in the inset of Fig. 3(a). The T_C value for SmNi$_2$Cd$_{20}$ is determined to be 6.6 K in zero magnetic field, which increases to T_C = 7.5 K in an applied magnetic field of H = 5 T. This behavior is consistent with a ferromagnetic ground state in SmNi$_2$Cd$_{20}$, in agreement with our magnetic susceptibility results.

In order to analyze the behavior of the electrical resistivity at low temperature, the $\rho(T)$ data were fit with a power law of the form $\rho = \rho_0 + AT^n$. The best-fit parameter values for ρ_0 (selected to maximize the linear region of the log($\rho - \rho_0$) vs. log$T$ fit extending from low T) and A are listed in Table I. As an example, a best fit for the SmNi$_2$Cd$_{20}$ data is plotted as a solid line in Fig. 3(c). The residual resistivity, ρ_0, increases with increasing magnetic field. For both H = 0 T and H = 5 T, $n \sim 3$ indicating that SmNi$_2$Cd$_{20}$ exhibits neither typical Fermi-liquid ($n \sim 2$) nor typical non-Fermi liquid ($n < 2$) behavior. On the other hand, the exponent values of $n \sim 2$ for SmFe$_2$Zn$_{20}$, SmRu$_2$Zn$_{20}$, and SmPd$_2$Cd$_{20}$ are consistent with

a Fermi-liquid state and $n \sim 0.9$ for $SmCo_2Zn_{20}$ is consistent with typical non-Fermi liquid behavior.[45,46] We note that these power-law fits were made to maximum temperatures that are less than the respective spin-wave gap temperatures Δ_{spw} (see Table I); therefore, scattering with spin-waves should be negligible in this analysis and can safely be neglected.

Since ferromagnetic order occurs below T_C, electron-spin wave scattering at higher temperatures was considered with the form[47],

$$\rho(T) = \rho_0 \ + \ B\frac{T}{\Delta_{spw}}(1+2\frac{T}{\Delta_{spw}})\exp(-\frac{\Delta_{spw}}{T}), \quad (3)$$

where Δ_{spw} is the spin-wave energy gap, which may result either from magnetic anisotropy or from broken symmetry due to the presence of a CEF. This formula describes the $\rho(T)$ data in a ferromagnetically-ordered state. A Fermi-liquid term AT^2 was added to Eq. (3) for fits to $SmFe_2Zn_{20}$ and $SmRu_2Zn_{20}$ data. An example of the best fit for $SmFe_2Zn_{20}$ is given in Fig. 3(d). As determined from the fits, the spin-wave energy gap values Δ_{spw} for $SmFe_2Zn_{20}$, $SmRu_2Zn_{20}$, and $SmNi_2Cd_{20}$ are 4.8 K, 3.9 K, and 8.8 K, respectively. However, $SmPd_2Cd_{20}$ orders antiferromagnetically so the following expression was used to fit the spin-wave scattering contribution to electrical resistivity[48,49],

$$\rho(T) = \rho_0 \ + \ AT^2 + C\Delta_{spw}^2\sqrt{\frac{T}{\Delta_{spw}}} \times \left[1+\frac{2}{3}\left(\frac{T}{\Delta_{spw}}\right)+\frac{2}{15}\left(\frac{T}{\Delta_{spw}}\right)^2\right]e^{-\frac{\Delta_{spw}}{T}}. \quad (4)$$

The differences in the values extracted for Δ_{spw} via fits to the low-temperature $\rho(T)$ data using Eqs. (3) and (4) are small because the exponential term that contains the gap in its argument is the dominant term in both expressions. However, the values for Δ_{spw} extracted by using Eq. (4) agree much better with the values for the energy gap obtained from fits of the low-temperature specific-heat data as discussed below. The spin-wave energy gap Δ_{spw} for $SmPd_2Cd_{20}$ is determined to be 3.6 K. Because magnetic order is not observed for $SmCo_2Zn_{20}$, it is inappropriate to describe the $\rho(T)$ data with an expression containing spin-wave scattering; therefore, we have limited these fits to the $\rho(T)$ data for $SmFe_2Zn_{20}$, $SmRu_2Zn_{20}$, $SmNi_2Cd_{20}$, and $SmPd_2Cd_{20}$. The extracted values for Δ_{spw} are reasonably close to one another and are listed in Table I.

Specific heat divided by temperature, C/T, vs. temperature T data are shown in Fig. 4(a). A sharp lambda-like anomaly in C/T is observed at T_C = 6.76 K for $SmRu_2Zn_{20}$, T_C = 6.34 K for $SmNi_2Cd_{20}$, and T_N = 3.05 K for $SmPd_2Cd_{20}$, indicating a second-order phase transition. However, C/T vs. T data do not manifest a standard lambda-like anomaly for $SmFe_2Zn_{20}$; rather, they exhibit a broad shoulder around T_C, which is taken to be the mid-point of the region with nearly zero slope, and was determined to be T_C = 44.4 K. This broad feature is observed more clearly after a background subtraction as shown in Fig. 4(c)-(e), which may indicate a distribution of T_C values associated with multiple transitions. All of the magnetic ordering temperatures are indicated by arrows in Fig. 4(a). The upturn in $SmCo_2Zn_{20}$ below 10 K may be related to a Schottky anomaly due to splitting of the Hunds's rule ground state of Sm^{3+} by the CEF. Similar results in $C(T)$ data for $SmCo_2Zn_{20}$ were observed by Jia *et al*.[19] Additionally, we observed another upturn at lower temperatures below 2 K which may also be related to a Schottky anomaly due to splitting of the nuclear states. On the other hand, this upturn might be associated with NFL behavior in $SmCo_2Zn_{20}$, which is supported by the sub-quadratic temperature dependence of the electrical resistivity below $\sim$ 2 K. Low-temperature specific heat measurements are necessary to clarify whether $SmCo_2Zn_{20}$ has a NFL or a FL ground state in which the properties below 10 K are dominated by spin-fluctuations. It is of interest to note that a broad shoulder below T_C and T_N is a common feature in compounds such as $TbCo_2Zn_{20}$, $ErFe_2Zn_{20}$, and $PrTi_2Al_{20}$.[19,50] According to calculation by Fishman and Liu,[51] these features arise naturally in a Heisenberg ferromagnet with large spin quantum number; however, it is also possible for quantum fluctuations in the transverse degrees of freedom to produce similar features.[51]

The electronic and phonon contributions to specific heat, characterized by γ and β, respectively, were determined by linear fits to the data plotted as C/T vs. T^2 using the expression $C/T = \gamma + \beta T^2$. The fits were performed in the 100-250 K^2 temperature range to avoid contributions from magnetic order below 10 K or Schottky anomalies for $SmCo_2Zn_{20}$, $SmRu_2Zn_{20}$, $SmNi_2Cd_{20}$, and $SmPd_2Cd_{20}$. The γ values of $SmCo_2Zn_{20}$, $SmRu_2Zn_{20}$, $SmNi_2Cd_{20}$, and $SmPd_2Cd_{20}$ are listed in Table II together with γ values for non-magnetic YFe_2Zn_{20}, YNi_2Cd_{20}, and $LaNi_2Cd_{20}$ reference compounds.[30,33] These values of γ are upper limits, and their precise values are subject to some uncertainty because of experimental constraints imposed by the low-temperature upturn of C/T for $SmCo_2Zn_{20}$ and the sharp lambda-like anomalies for $SmRu_2Zn_{20}$, $SmNi_2Cd_{20}$, and $SmPd_2Cd_{20}$. An example of the linear fit for $SmFe_2Zn_{20}$ is shown in Fig. 4(b) as a solid line; the fit was performed in the 4-25 K^2 temperature range. Sommerfeld coefficient values of $\gamma \sim$ 57 mJ/mol-K^2 for $SmFe_2Zn_{20}$, $\sim$ 79.5 mJ/mol-K^2 for $SmCo_2Zn_{20}$, $\sim$ 258 mJ/mol-K^2 for $SmRu_2Zn_{20}$, $\sim$ 165 mJ/mol-K^2 for $SmNi_2Cd_{20}$, and $\sim$ 208 mJ/mol-K^2 for $SmPd_2Cd_{20}$ were obtained.

In general, γ is proportional to the total density of states at the Fermi energy, $D(E_f)$. The observed differences between γ values probably simply reflect differences in the electronic structure of these compounds. On average, the compounds with X = Cd appear to have larger values of γ than when X = Zn, and the γ values also seem to increase when we go from $3d$ to $4d$ transition metal elements. For clarity, it would be helpful to perform band structure calculations. Since there are 23 atoms per formula unit in these 1-2-20 compounds, the electronic states coming from the transition metal and Zn or Cd ions could produce a fairly large contribution to $D(E_f)$ without considering any Sm contributions. We have, therefore, compared the γ values we measure for the Sm-based compounds with values obtained from suitable non-magnetic reference compounds where R = Y

TABLE II: Summary of characteristic quantities and ratios for RTr_2Zn_{20} (R = Y, La, Sm, Tr = Fe, Co, Ru) and RTr_2Cd_{20} (R = Y, La, Sm, Tr = Ni, Pd). Included in the table are the Sommerfeld coefficient of the specific heat, γ; Sommerfeld-Wilson ratio, SWR; and Kadowaki-Woods ratio, KWR.

Compound	γ, ($\frac{\mathrm{mJ}}{\mathrm{mol-K^2}}$)	SWR	KWR, ($\frac{\mu\Omega\mathrm{cmmol^2K^2}}{\mathrm{mJ^2}}$)
YFe_2Zn_{20}	53		
YNi_2Cd_{20}	22.9		
$LaNi_2Cd_{20}$	25.9		
$SmFe_2Zn_{20}$	57		
$SmCo_2Zn_{20}$	79.5		
$SmRu_2Zn_{20}$	258	2.0	4.4×10^{-7}
$SmNi_2Cd_{20}$	165		
$SmPd_2Cd_{20}$	208	0.7	1.1×10^{-5}

or La. The difference between these values is a measure of the contribution of Sm and its interactions with itinerant electron states (i.e., any quasiparticle resonances) to $D(E_f)$. The electronic specific heat coefficient, γ, (see Table II) for $SmFe_2Zn_{20}$ and $SmCo_2Zn_{20}$ is not very different from the γ value of non-magnetic YFe_2Zn_{20}. However, there is an enhancement of the γ value for $SmRu_2Zn_{20}$, $SmNi_2Cd_{20}$, and $SmPd_2Cd_{20}$ relative to the γ value of YRu_2Zn_{20} ($\gamma \sim 34$ mJ/mol-K^2),[22] YFe_2Zn_{20}, YNi_2Cd_{20}, and $LaNi_2Cd_{20}$, indicating an enhancement of $D(E_f)$ associated with Sm ions. The Debye temperature, Θ_D, was calculated using the relation: $\Theta_D = (23 * 1944 * 1000(1/\beta))^{1/3}$ K. For all of the compounds studied, Θ_D values are roughly the same near $\sim$ 214 K.

Figure 4(c) displays the magnetic contribution to specific heat, $\Delta C(T)$, of $SmFe_2Zn_{20}$ as a representative example. $\Delta C(T)$ is obtained after the specific heat of nonmagnetic YFe_2Zn_{20}, $LaNi_2Cd_{20}$ (used to estimate the lattice contribution to specific heat for $SmFe_2Zn_{20}$ and $SmNi_2Cd_{20}$, respectively.) is subtracted from the specific heat of $SmFe_2Zn_{20}$ and $SmNi_2Cd_{20}$, respectively, and $\gamma T + \beta T^3$ (estimated electronic and lattice contribution terms) is subtracted from the specific heats of $SmRu_2Zn_{20}$ and $SmPd_2Cd_{20}$. The low-temperature data for $SmFe_2Zn_{20}$, $SmRu_2Zn_{20}$, and $SmNi_2Cd_{20}$ were fit with a spin-wave formula $\Delta C(T) \propto T^n$, which is appropriate for magnetically isotropic metals. Fits were made using $\Delta C(T) \propto T^{3/2}\exp(-\Delta_{spw}/T)$ for magnetically anisotropic metals, and $\Delta C(T) \propto T^3\exp(-\Delta_{spw}/T)$ for $SmPd_2Cd_{20}$.[52] From the first formula, we obtained exponent values of *n* $\sim$ 3.1, 3.11, 2.8, and 2.9 for $SmFe_2Zn_{20}$, $SmRu_2Zn_{20}$, $SmNi_2Cd_{20}$, and $SmPd_2Cd_{20}$, respectively. These values for $SmFe_2Zn_{20}$, $SmRu_2Zn_{20}$, and $SmNi_2Cd_{20}$ are in disagreement with predictions from theoretical calculations involving ferromagnetic spin waves which yield a $T^{3/2}$ dependence, but they are consistent with a calculation for the specific heat that involves antiferromagnetic spin waves which gives $C \propto T^3$.[53] The spin-wave energy gap Δ_{spw} values were determined from the second formula to be 7.0 K, 4.9 K, 10.8 K, and 5.7 K for $SmFe_2Zn_{20}$, $SmRu_2Zn_{20}$, $SmNi_2Cd_{20}$, and $SmPd_2Cd_{20}$, respectively. These values are consistent (i.e., of the same order of magnitude) with the values of 4.8 K, 3.9 K, 8.8 K, and 3.6 K, which were determined from the zero-field electrical resistivity data.

The magnetic contribution to specific heat, $\Delta C(T)$, of $SmCo_2Zn_{20}$, $SmRu_2Zn_{20}$, $SmNi_2Cd_{20}$, and $SmPd_2Cd_{20}$ is displayed in Fig. 4(d) (left axis). The magnetic contribution to the entropy, $S_{mag} = \int(\Delta C/T)dT$, (extrapolating a power-law T-dependence of $\Delta C/T$ to 0 K to estimate the magnetic entropy below 1.8 K) is displayed in Fig. 4(d) (corresponding to the right axis). The entropy, S_{mag}, attains a value of $S_{mag} \sim 5.95$ J mol^{-1} K^{-1} for $SmRu_2Zn_{20}$, $S_{mag} \sim 12.8$ J mol^{-1} K^{-1} for $SmNi_2Cd_{20}$, and $S_{mag} \sim 7.81$ J mol^{-1} K^{-1} for $SmPd_2Cd_{20}$ at their respective magnetic ordering temperatures. Then S_{mag} reaches a value of 9.14 J mol^{-1} K^{-1} and 8.1 J mol^{-1} K^{-1} by 15 K and saturates for $SmCo_2Zn_{20}$ and $SmRu_2Zn_{20}$, respectively. These values are lower than expected for Sm^{3+} with J = 5/2 ($S_{mag} = R\ln(2J+1) = 14.9$ J mol^{-1} K^{-1}) with full degeneracy, but S_{mag} reaches $\sim R\ln 2$ at T_C = 6.76 K, which suggests that the ground state of Sm for $SmRu_2Zn_{20}$ could be a Γ_7 doublet; however, low-temperature specific heat measurements are necessary to identify the ground state for $SmCo_2Zn_{20}$, because of the low temperature upturn below 10 K. On the other hand, $S_{mag} \sim 14.7$ J mol^{-1} K^{-1} at 15 K for $SmNi_2Cd_{20}$ nearly reaches $R\ln 6$, indicating that the expected magnetic entropy is completely recovered by this temperature. A value of $S_{mag} \sim 11.7$ J mol^{-1} K^{-1} at 15 K for $SmPd_2Cd_{20}$ and a value of 7.81 J mol^{-1} K^{-1} at T_N = 3.4 K suggests that the ground state of Sm in this compound is probably a Γ_8 quartet.[54] Thus, our check demonstrates that the estimated $\Delta C/T$ curves for the SmTr_2Zn_{20} (*Tr* = Fe, Co, Ru) and SmTr_2Cd_{20} (*Tr* = Ni, Pd) compounds are reasonable. The sizable release of magnetic entropy indicates that the valence of Sm ions is close to 3+. On the other hand, S_{mag} vs. T for $SmFe_2Zn_{20}$, displayed in Fig. 4(e), attains a value 18.7 J mol^{-1} K^{-1} above the ferromagnetic transition. This is a larger value than expected for Sm^{3+}, which may be due to a contribution from Fe ions to the magnetic entropy. Such a scenario is in concert with the larger μ_{eff} value for $SmFe_2Zn_{20}$ than expected for the Sm^{3+} ion alone.

IV. DISCUSSION

The magnetic, electrical transport, and thermodynamic properties of $SmFe_2Zn_{20}$, $SmRu_2Zn_{20}$, and $SmNi_2Cd_{20}$ reveal ferromagnetic order below T_C = 47.4 K, 7.6 K, and 7.5 K, respectively. Antiferromagnetic order is observed below T_N = 3.4 K for $SmPd_2Cd_{20}$, but no evidence for magnetic order is observed down to 110 mK for $SmCo_2Zn_{20}$. Magnetic order with low transition temperatures or no ordering at all might be expected in the RTr_2Zn_{20} series of compounds due to their very low rare-earth ion concentrations and large spatial separations between neighboring R ions. However, $SmFe_2Zn_{20}$ exhibits a relatively high-Curie temperature of T_C = 47.4 K. In the RTr_2Zn_{20} compounds, the rare-earth and transition-metal ions are surrounded by Zn cages preventing direct magnetic exchange interactions between the 4*f* or 3*d* electrons; however, 3*d* electrons from Fe sites in RFe$_2$Zn$_{20}$

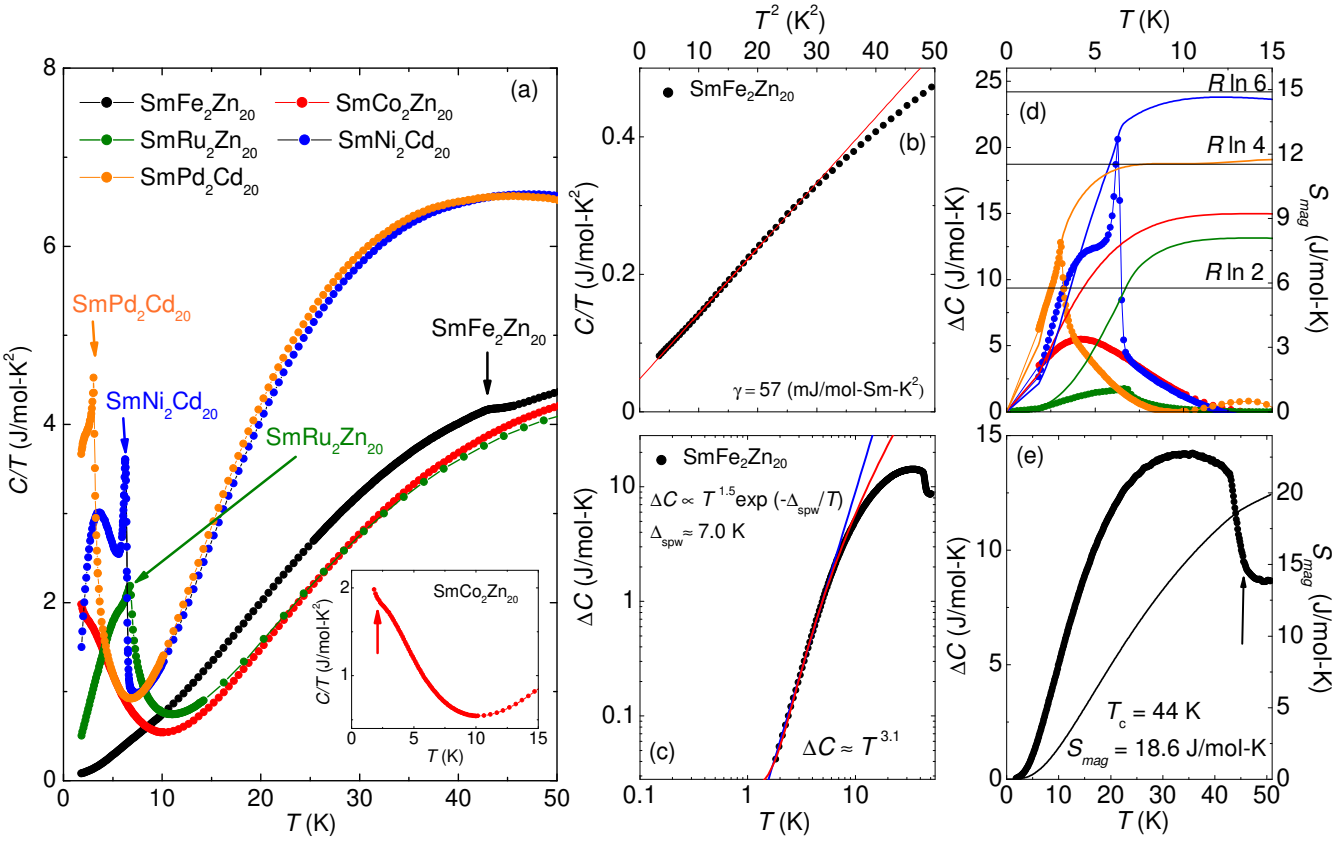

FIG. 4: (a) Specific heat divided by temperature, C/T, for SmTr_2Zn$_{20}$ (Tr = Fe, Co, Ru) and SmNi$_2$Cd$_{20}$ in zero magnetic field. Arrows refer to magnetic phase transition temperatures. Inset: C/T for SmCo$_2$Zn$_{20}$ emphasizing the upturn at low temperatures below 2 K (indicated by the arrow). (b) C/T vs. T^2 for SmFe$_2$Zn$_{20}$. The solid line represents a fit to the data using the equation $C/T = \gamma + \beta T^2$. (c) Logarithmic plot of power-law fit (blue solid line) and anisotropic spin-wave fit (red solid line) to the magnetic contribution to the specific heat, $\Delta C(T)$, for SmFe$_2$Zn$_{20}$ after electronic and lattice contributions have been subtracted. (d) Magnetic entropy, S_{mag}, vs. T for SmTr_2Zn$_{20}$ (Tr = Co, Ru) and SmNi$_2$Cd$_{20}$. (e) Magnetic contribution to specific heat, ΔC, (corresponds to left axis) and the magnetic entropy, S_{mag}, (right axis) vs. T for SmFe$_2$Zn$_{20}$.

act as important mediators via the RKKY interaction and the indirect magnetic exchange interaction between Fe 3d electrons enhances the magnetic interactions between R^{3+} localized magnetic moments, resulting in the remarkably high T_C for RFe$_2$Zn$_{20}$ compounds. It has also been suggested that the magnetic exchange interaction between the two R ions is weaker than that between R and Fe ions.[55] In this scenario, the T_C of RFe$_2$Zn$_{20}$ compounds is enhanced by the magnetic exchange interaction between R and Fe ions.[55] The T_C values in the RFe$_2$Zn$_{20}$ series of compounds with R = Gd-Lu are reported to scale with the de Gennes factor,[56] and the relatively high T_C value we observe for SmFe$_2$Zn$_{20}$ fits in with this scaling behavior of the heavier rare-earth ion members. We note that RTr_2Zn$_{20}$ compounds with Tr = Ru, Os, which are both in the same column as Fe, are characterized by significantly lower T_C values compared to those for Tr = Fe.[19] In the neighboring column, the RTr_2Zn$_{20}$ compounds with Tr = Co, Rh, Ir are known to order antiferromagnetically.[19] Therefore, it appears that the number of conduction electrons from the transition-metal d-electron shell plays an important role in determining the magnetic properties of the RTr_2Zn$_{20}$ compounds. However, this conclusion does not appear to apply for all the RTr_2Cd$_{20}$ compounds because, even though Ni and Pd both reside in the same column of the periodic table, SmNi$_2$Cd$_{20}$ orders ferromagnetically with T_C = 7.5 K while SmPd$_2$Cd$_{20}$ has an antiferromagnetic ground state with T_N = 3.4 K. Calculations of the electronic band structure would be helpful to understand why the magnetic structures for SmNi$_2$Cd$_{20}$ and SmPd$_2$Cd$_{20}$ are different.

The electronic specific heat coefficient, γ, (see values of γ listed in Table II) for SmFe$_2$Zn$_{20}$ and SmCo$_2$Zn$_{20}$ is not significantly larger than the γ value for non-magnetic YFe$_2$Zn$_{20}$ and YCo$_2$Zn$_{20}$ ($\gamma \sim 18.3$ mJ/mol-K^2)[22]. This observation suggests that the electronic structure and the well-localized nature of 4f electrons are quite similar in these compounds. However, an enhancement of the γ value for SmRu$_2$Zn$_{20}$, SmNi$_2$Cd$_{20}$, and SmPd$_2$Cd$_{20}$, relative to the γ values for YRu$_2$Zn$_{20}$ ($\gamma \sim 34$ mJ/mol-K^2),[22] YNi$_2$Cd$_{20}$, and LaNi$_2$Cd$_{20}$, suggests that heavy quasiparticles form at low temperature or that there is a peak in the electronic density of states $D(E)$ near E_F contributed by Sm states. Since we were unable to prepare non-magnetic reference compounds

for $SmPd_2Cd_{20}$, YPd_2Cd_{20} or $LaPd_2Cd_{20}$, we assumed that the density of states of YNi_2Cd_{20}, $LaNi_2Cd_{20}$, YPd_2Cd_{20}, and $LaPd_2Cd_{20}$ are similar. Values of γ that are significantly enhanced relative to those of non-magnetic analogues imply that the f-electrons are strongly admixed with conduction-electron states and have developed delocalized character. However, the value $n \sim 3$ of the exponent from the power-law fit of the electrical resistivity data for $SmNi_2Cd_{20}$ and the localized character of f electrons (determined from $\mu_{eff}/\mu_{sat} \sim 1$)[44] in $SmRu_2Zn_{20}$ and $SmNi_2Cd_{20}$ are inconsistent with typical heavy fermion (HF) physics. Localized f electrons in $SmRu_2Zn_{20}$ and $SmNi_2Cd_{20}$ participate in their respective FM ground states via the RKKY interaction,[39–41] which competes with the heavy fermion state in a generic Doniach model context. This contradictory behavior of $SmRu_2Zn_{20}$ and $SmNi_2Cd_{20}$ suggests that these compounds may be near a ferromagnetic quantum critical point (QCP). Due to the possible proximity to a ferromagnetic QCP, $SmRu_2Zn_{20}$ and $SmNi_2Cd_{20}$ compounds represent potential new model systems for studying the break down of Fermi-Liquid (FL) behavior near a ferromagnetic QCP. Even though there are extensive studies on HF systems that focus on antiferromagnetic (AFM) QCP's, there are a limited but increasing number of HF ferromagnets (FM's). In particular, Sm-based HF FMs are rare and include $SmFe_4P_{12}$ ($\gamma \sim$ 350 mJ/mol-K^2),[11] $SmOs_4Sb_{12}$ ($\gamma \sim$ 880 mJ/mol-K^2),[9] and SmPtSi ($\gamma \sim$ 250 mJ/mol-K^2).[57] We also note that a few other Sm-based compounds with the $CeCr_2Al_{20}$-type structure are considered to be heavy fermions with $\gamma \sim$ 100 mJ/mol-K^2 for $SmTi_2Al_{20}$, $\gamma \sim$ 720 mJ/mol-K^2 for SmV_2Al_{20}, and $\gamma \sim$ 1000 mJ/mol-K^2 for $SmCr_2Al_{20}$, which all have AFM ground states.[31,32] The investigation of other FM compounds near a QCP is therefore highly desirable for a more complete understanding of quantum criticality. An enhanced electronic specific heat coefficient for $SmPd_2Cd_{20}$, which has as exponent value of $n \sim 2$, an AFM ground state, and a possible metamagnetic transition at T = 2 K and $H \sim$ 2.5 T supports an interpretation that this compound is near a QCP with a FL ground state. We want to emphasize that there is no evidence for a coherence temperature in the electrical resistivity data, as would be expected for typical HF compounds. On the other hand, this lack of distinct features in the electrical resistivity $\rho(T)$ has been observed in other Sm-based HF compounds such as $SmFe_4P_{12}$ and $SmOs_4Sb_{12}$,[9,11] and may indicate that the HF composite quasiparticles in these compounds develop through a route different from the standard Kondo-lattice mechanism.

In order to elucidate the character of the HF behavior, we calculated the Kadowaki-Woods ratio, KWR = A/γ^2, where γ is the coefficient of the electronic specific heat and A is the coefficient of the T^2 contribution to the electrical resistivity.[58] Calculations were performed for the compounds that have a quadratic T dependence at low temperature in electrical resistivity data. Calculated KWR values are given in Table II. In the original treatment,[58] KWR $\approx 10^{-5}$ $\frac{\mu\Omega\mathrm{cmmol}^2\mathrm{K}^2}{\mathrm{mJ}^2}$, which is almost the same value we calculate for $SmPd_2Cd_{20}$. More recently, it has been found that a number of HF compounds based on lanthanide or actinide ions other than Ce (e.g., Sm, Eu, Yb, U) exhibit KWR values closer to A/γ^2 = 1.0 $\times$ 10^{-6}, which can be explained by taking into account the degeneracy, N, of the lanthanide or actinide ions.[59] For $SmRu_2Zn_{20}$, KWR is close to 0.36 $\times$ 10^{-6} when we assume N = 8, supporting the formation of a magnetic FL ground state. Moreover, we consider the Sommerfeld-Wilson ratio, SWR = $(\pi^2 k_B^2/(\mu_{eff})^2)\chi_0/\gamma$, where k_B is the Boltzmann constant, μ_{eff} is the effective magnetic moment, and χ_0 is the enhanced Pauli susceptibility.[60] SWR values are tabulated in Table II. An SWR ratio value of 0.7 is calculated for $SmPd_2Cd_{20}$; this value is very close to 1, which is expected for a free electron gas.[61] We calculate, a value of 2 for $SmRu_2Zn_{20}$, which is consistent with a Kondo system and has been observed in many HF systems. The f electron spin fluctuations presumably enhance χ_0 relative to γ, which leads to larger value for the SWR.[61,62]

Low-temperature electrical resistivity data suggest the presence of spin-wave excitations below T_C for $SmFe_2Zn_{20}$, $SmRu_2Zn_{20}$, and $SmNi_2Cd_{20}$, and below T_N for $SmPd_2Cd_{20}$. The uncertainty in the ground state of the Sm multiplet energy-level scheme and the microscopic properties of spin-wave excitations may be resolved by performing neutron scattering experiments. However, for such an experiment, it should be noted that both Sm and Cd are strong neutron absorbers; therefore, samples would need to be synthesized using one of the less-absorbing Sm isotopes like ^{152}Sm or ^{154}Sm and a Cd isotope like ^{114}Cd.[63]

V. SUMMARY

Measurements of electrical resistivity, magnetization, and specific heat have been performed for single crystals of the caged compounds $SmTr_2Zn_{20}$ (Tr = Fe, Co, Ru) and $SmTr_2Cd_{20}$ (Tr = Ni, Pd). $SmFe_2Zn_{20}$, $SmRu_2Zn_{20}$, and $SmNi_2Cd_{20}$ exhibit ferromagnetic order with Curie temperatures of T_C = 47.4 K, 7.6 K, and 7.5 K, respectively, while $SmPd_2Cd_{20}$ is an antiferromagnet with T_N = 3.4 K. No evidence for magnetic order is observed in $SmCo_2Zn_{20}$ down to 110 mK. Sommerfeld coefficients, γ, of 57 mJ/mol-K^2 for $SmFe_2Zn_{20}$, 79.5 mJ/mol-K^2 for $SmCo_2Zn_{20}$, 258 mJ/mol-K^2 for $SmRu_2Zn_{20}$, 165 mJ/mol-K^2 for $SmNi_2Cd_{20}$, and 208 mJ/mol-K^2 for $SmPd_2Cd_{20}$ are obtained. Enhanced Sommerfeld coefficients relative to non-magnetic reference compounds and the exponent $n \sim 2$ from the power-law fits of electrical resistivity data for $SmRu_2Zn_{20}$ and $SmPd_2Cd_{20}$ suggest an enhancement of the quasiparticle masses related due to hybridization between localized $4f$ and conduction electron states. Therefore, we suggest that $SmRu_2Zn_{20}$ is a new addition to the rare class of Sm-based HF ferromagnet with a KWR value of 4.4 $\times$ 10^{-7} and an SWR value of 2, which have been observed in many HF Kondo lattice systems.

Acknowledgments

Research at UCSD was supported by the U. S. Department of Energy, Office of Basic Energy Sciences, Division of Mate-

rial Sciences and Engineering under Grant No. DE-FG02-04-ER46105 (sample synthesis and physical properties measurements above 1 K), and the National Science Foundation under Award Grant No. DMR 1206553 (Physical properties measurements below 1 K). Research at California State University, Fresno is supported by the National Science Foundation under Grant No. DMR 1104544. Helpful discussions with Prof. Tatsuya Yanasigawa are gratefully acknowledged.

* Corresponding Author: mbmaple@ucsd.edu

[1] A. Jayaraman, V. Narayanamurti, E. Bucher, and R. G. Maines, Phys. Rev. Lett. **25**, 1430 (1970).

[2] M. B. Maple and D. Wohlleben, Phys. Rev. Lett. **27**, 511 (1971), AIP Conf. Proc., No. 18, edited by C. D. Graham, Jr. and J. J. Rhyne, p. 447 (1974).

[3] S. Bakanowski, J. Crow, and T. Mihalisin, Solid State Commun. **22**, 241 (1977).

[4] L. De Long, R. McCallum, W. Fertig, M. Maple, and J. Huber, Solid State Commun. **22**, 245 (1977).

[5] A. Menth, E. Buehler, and T. H. Geballe, Phys. Rev. Lett. **22**, 295 (1969).

[6] H. Kotegawa, H. Hidaka, Y. Shimaoka, T. Miki, T. C. Kobayashi, D. Kikuchi, H. Sugawara, and H. Sato, J. Phys. Soc. Jpn. **74**, 2173 (2005).

[7] S. Sanada, Y. Aoki, H. Aoki, A. Tsuchiya, D. Kikuchi, H. Sugawara, and H. Sato, J. Phys. Soc. Jpn. **74**, 246 (2005).

[8] A. Yamasaki, S. Imada, H. Higashimichi, H. Fujiwara, T. Saita, T. Miyamachi, A. Sekiyama, H. Sugawara, D. Kikuchi, H. Sato, et al., Phys. Rev. Lett. **98**, 156402 (2007).

[9] M. Mizumaki, S. Tsutsui, H. Tanida, T. Uruga, D. Kikuchi, H. Sugawara, and H. Sato, J. Phys. Soc. Jpn. **76**, 053706 (2007).

[10] W. M. Yuhasz, N. A. Frederick, P.-C. Ho, N. P. Butch, B. J. Taylor, T. A. Sayles, M. B. Maple, J. B. Betts, A. H. Lacerda, P. Rogl, et al., Phys. Rev. B **71**, 104402 (2005).

[11] N. Takeda and M. Ishikawa, Journal of Physics: Condensed Matter **15** (2003).

[12] M. Yoshizawa, Y. Nakanishi, M. Oikawa, C. Sekine, I. Shirotani, S. R. Saha, H. Sugawara, and H. Sato, J. Phys. Soc. Jpn. **74**, 2141 (2005).

[13] S. Niemann and W. Jeitschko, J. Sol. State Chem. **144**, 337 (1995).

[14] T. Nasch, W. Jeitschko, and U. C. Rodewald, Z. Naturforsch. **52 b**, 1023 (1997).

[15] V. M. Thiede, W. Jeitschko, S. Niemann, and T. Ebel, Journal of Alloys and Compounds **267**, 23 (1998).

[16] P. Kripyakevich and O. Zarechnyuk, Dopov. Akad. Nauk Ukr. RSR **Ser. A**, 364 (1968).

[17] O. Moze, L. Tung, J. Franse, and K. Buschow, Journal of Alloys and Compounds **268**, 39 (1998).

[18] F. C. Frank and J. S. Kasper, Acta Crystallographica **11**, 184 (1958).

[19] S. Jia, N. Ni, S. L. Bud'ko, and P. C. Canfield, Phys. Rev. B **80**, 104403 (2009).

[20] Y. Isikawa, T. Mizushima, K. Kumagai, and T. Kuwai, J. Phys. Soc. Jpn. **82**, 083711 (2013).

[21] S. Jia, S. L. Bud'ko, G. D. Samolyuk, and P. C. Canfield, Nature Physics **3**, 334 (2007).

[22] S. Jia, N. Ni, S. L. Bud'ko, and P. C. Canfield, Phys. Rev. B **76**, 184410 (2007).

[23] T. Onimaru, K. T. Matsumoto, Y. F. Inoue, K. Umeo, Y. Saiga, Y. Matsushita, R. Tamura, K. Nashimoto, I. Ishii, T. Suzuki, et al., J. Phys. Soc. Jpn. **79**, 033704 (2010).

[24] A. Sakai and S. Nakatsuji, J. Phys. Soc. Jpn. **80**, 063701 (2011).

[25] A. Sakai, K. Kuga, and S. Nakatsuji, J. Phys. Soc. Jpn. **81**, 083702 (2012).

[26] T. J. Sato, S. Ibuka, Y. Nambu, T. Yamazaki, T. Hong, A. Sakai, and S. Nakatsuji, Phys. Rev. B **86**, 184419 (2012).

[27] Y. Saiga, K. Matsubayashi, T. Fujiwara, M. Kosaka, S. Katano, M. Hedo, T. Matsumoto, and Y. Uwatoko, J. Phys. Soc. Jpn. **77**, 053710 (2008).

[28] K. Matsubayashi, T. Tanaka, A. Sakai, S. Nakatsuji, Y. Kubo, and Y. Uwatoko, Phys. Rev. Lett. **109**, 187004 (2012).

[29] P. C. Canfield, S. Jia, E. D. Mun, S. L. Bud'ko, G. D. Samolyuk, and M. S. Torikachvili, Physica B **403**, 844 (2008).

[30] M. S. Torikachvili, S. Jia, E. D. Mun, S. T. Hannahs, R. C. Black, W. K. Neils, D. Martien, S. L. Bud'ko, and P. C. Canfield, Proceedings of the National Academy of Sciences **104**, 9960 (2007).

[31] A. Sakai and S. Nakatsuji, Phys. Rev. B **84**, 201106 (2011).

[32] R. Higashinaka, T. Maruyama, A. Nakama, R. Miyazaki, Y. Aoki, and H. Sato, J. Phys. Soc. Jpn. **80**, 093703 (2011).

[33] V. W. Burnett, D. Yazici, B. D. White, N. R. Dilley, A. J. Friedman, B. Brandom, and M. B. Maple, J. Solid. State Chem. **215**, 114 (2014).

[34] A. C. Larson and R. B. Von Dreele, *General Structure Analysis System (GSAS)* (2000).

[35] B. H. Toby, J. Appl. Crystallogr. **34**, 210 (2001).

[36] S. Jia, N. Ni, G. D. Samolyuk, A. Safa-Sefat, K. Dennis, H. Ko, G. J. Miller, S. L. Bud'ko, and P. C. Canfield, Phys. Rev. B **77**, 104408 (2008).

[37] W. Tian, A. D. Christianson, J. L. Zarestky, S. Jia, S. L. Bud'ko, P. C. Canfield, P. M. B. Piccoli, and A. J. Schultz, Phys. Rev. B **81**, 144409 (2010).

[38] J. J. M. Franse and R. J. Radwanski, *Handbook of Magnetic Materials*, vol. 7 (Elsevier, Amsterdam, 1993), edited by K. H. J. Buschow.

[39] M. A. Ruderman and C. Kittel, Phys. Rev. **96**, 99 (1954).

[40] T. Kasuya, Progress of Theoretical Physics **16**, 45 (1956).

[41] K. Yosida, Phys. Rev. **106**, 893 (1957).

[42] H. Hamaker, L. Woolf, H. MacKay, Z. Fisk, and M. Maple, Solid State Commun. **32**, 289 (1979).

[43] J. H. Van Vleck, *The Theory of Electric and Magnetic Susceptibilities* (Oxford University Press, London, 1932).

[44] P. Rhodes and E. P. Wohlfarth, Proc. R. Soc. A **273**, 247 (1963).

[45] M. B. Maple, Physica B **215**, 110 (1995).

[46] M. B. Maple, M. C. de Andrade, J. Herrmann, Y. Dalichaouch, D. A. Gajewski, C. L. Seaman, R. Chau, R. Movshovich, M. C. Aronson, and R. Osborn, J. Low Temp. Phys. **99**, 223 (1995).

[47] N. H. Franse, *Crystalline Electrical Field and Structural Effects in f-Electron Systems* (Plenum, New York, 1980), edited by J. E. Crow, R. P. Guertin, and T. W. Mihalisin.

[48] N. Hessel Andersen and H. Smith, Phys. Rev. B **19**, 384 (1979).

[49] M. B. Fontes, J. C. Trochez, B. Giordanengo, S. L. Bud'ko, D. R. Sanchez, E. M. Baggio-Saitovitch, and M. A. Continentino, Phys. Rev. B **60**, 6781 (1999).

[50] M. J. Kangas, D. C. Schmitt, A. Sakai, S. Nakatsuji, and J. Y. Chan, J. Sol. State Chem. **196**, 274 (2012).

[51] R. S. Fishman and S. H. Liu, Phys. Rev. B **40**, 11028 (1989).

[52] A. Mackintosh, Physics Letters **4**, 140 (1963).

[53] J. Van Kranendonk and J. H. Van Vleck, Rev. Mod. Phys. **30**, 1 (1958).

[54] K. R. Lea, M. J. M. Leask, and W. P. Wolf, J. Phys. Chem. Solids **23**, 1381 (1962).

[55] Y. Isikawa, T. Mizushima, S. Miyamoto, K. Kumagai, M. Nakahara, H. Okuyama, T. Tayama, T. Kuwai, and P. Lejay, J. Kor. Phys. Soc. **63**, 644 (2013).

[56] P. G. De Gennes, J. Phys. Radium **23**, 510 (1962).

[57] S. Ramakrishnan, K. Ghosh, A. D. Chinchure, V. R. Marathe, and G. Chandra, Phys. Rev. B **52**, 6784 (1995).

[58] K. Kadowaki and S. Woods, Solid State Commun. **58**, 507 (1986).

[59] N. Tsujii, H. Kontani, and K. Yoshimura, Phys. Rev. Lett. **94**, 057201 (2005).

[60] P. Gegenwart, J. Custers, Y. Tokiwa, C. Geibel, and F. Steglich,

Phys. Rev. Lett. **94**, 076402 (2005).
[61] Z. Fisk, H. R. Ott, and G. Aeppli, Jpn. J. Appl. Phys. **26**, 1882 (1987).
[62] Z. Fisk, H. R. Ott, and J. L. Smith, Nature **320**, 124 (1986).
[63] J.-H. Chung, M. Matsuda, S.-H. Lee, K. Kakurai, H. Ueda, T. J. Sato, H. Takagi, K.-P. Hong, and S. Park, Phys. Rev. Lett. **95**, 247204 (2005).